Horizontal Inhomogeneity in the D-Region Ionosphere During an X-Class Solar Flare Determined by OCTAVE VLF Observations

Masaharu Nakayama, Hiroyo Ohya, Fuminori Tsuchiya, Kenro Nozaki, Kazuo Shiokawa, and Hiroyuki Nakata

Abstract – In this study, horizontal inhomogeneity in electron density in the D-region ionosphere during an X-class solar flare was investigated using multipath very low-frequency (VLF, 3 kHz to 30 kHz)/low-frequency (LF, 30 kHz to 300 kHz) transmitter signals of the worldwide OCTAV0...
E (Observation of CondiTion of ionized Atmosphere by VLF Experiment) network. During an X-class solar flare that occurred at 08:57 UT on 6 September 2017, the variations in VLF/LF amplitude (ΔA) and phase (ΔP) at midlatitudes in the Asian sector were 2.65 dB to 14.73 dB and 31.0° to 150.25°, respectively. The reflection height generally decreased during the solar flare, consistent with an increase in electron density in the D-region ionosphere. Based on the wave-hop method and assuming a reference height in consideration of sunset effects, the amplitude of the variation in the reflection height (Δh) was estimated to be 1.0 km to 4.8 km. The Δh of paths close to the subsolar point was larger than that of distant paths. Based on the International Reference Ionosphere (IRI-2016) model, the variation in electron density (ΔN) at χ (the solar zenith angle) = 64.34° was larger (5465.7 cm^{-3}) than that at $\chi = 80.18°$ (200.4 cm^{-3}) at a height of 85 km. Thus, our results indicate that the inhomogeneity in D-region ionization was due to the solar flare.

1. Introduction

During solar flares, both the amplitude and the phase of very low-frequency (VLF, 3 kHz to 30 kHz)/low-frequency (LF, 30 kHz to 300 kHz) transmitter signals change due to large X- and ultraviolet rays [1]. In previous studies, an increase in electron density in the D-region ionosphere during solar flares was estimated from the ionospheric reference height $H'$and rate of increase in electron density at height β of Wait's parameters, which were in turn estimated from observed narrowband VLF transmitter signals [2]. Electron density in the D-region ionosphere was larger at the solar minimum than at the solar maximum for the same class of solar flares. Solar activities also influence the minimum X-ray flux (the lower-range value changed according to the D-region ionosphere due to solar flares), which is large at the solar maximum and small at the solar minimum. This implies that the response of the D-region ionosphere to solar flares is more sensitive at the solar minimum.

The horizontal distribution of the reflection height and electron density during solar flares is unknown. Thus, in this study, we investigated the horizontal inhomogeneity of the reflection height and electron density in the D-region ionosphere during the X2.2-class solar flare that occurred at 08:57 UT on 6 September 2017, using multipath VLF/LF transmitter signals of the OCTAVE (Observation of CondiTion of ionized Atmosphere by VLF Experiment) network.

Manuscript received 26 December 2022.

Masaharu Nakayama, Hiroyo Ohya, and Hiroyuki Nakata are with the Graduate School of Science and Engineering, Chiba University, 1-33 Yayoi-cho, Inage-ku, Chiba 263-8522, Japan; e-mail: mrakn_tech@chiba-u.jp, ohya@faculty.chiba-u.jp, nakata@faculty.chiba-u.jp.

Fuminori Tsuchiya is with the Planetary Plasma and Atmospheric Research Center (PPARC), Graduate School of Science, Tohoku University, Aramaki-aza-aoba 6-3, Aoba, Sendai, Miyagi 980-8578, Japan; e-mail: tsuchiya@pparc.gp.tohoku.ac.jp.

Kenro Nozaki is with the University of Electro-Communications, 1-5-1 Chofugaoka, Chofu, Tokyo 182-8585, Japan; e-mail: kuboken@za2.so-net.ne.jp.

Kazuo Shiakawa is with the Institute for Space-Earth Environmental Research (ISEE), Nagoya University, Furo-cho, Chikusa-ku, Nagoya 464-8601, Japan; e-mail: shiokawa@isee.nagoya-u.ac.jp.

2. Observations and the Wave-Hop Method

Figure 1 shows the location of 1) the subsolar point and 2) the VLF/LF paths. Four transmitters (NWC [19.8 kHz, Australia], JJI [22.2 kHz, Japan], JJY [40 kHz and 60 kHz, Japan], and BPC [68.5 kHz, China]) and three receivers (RKB [43.45°N, 143.77°E, Rikubetsu, Japan], KAG [31.59°N, 130.55°E, Kagoshima, Japan], and PKR [65.125°N, 147.488°W, Poker Flat, USA]) were used in this study. The antennas were monopole antennas sensitive to electric field components. The amplitude and phase of the VLF/LF waves were received at a 0.1-s sampling rate. Thirteen VLF/LF paths were analyzed in total. Table 1 shows the solar zenith angle at the midpoints of all paths.

Variations in amplitude (ΔA) and phase (ΔP) corresponding to the difference between the peak value and background level were analyzed, as shown in Figure 2.

The wave-hop method was used to estimate the decrease in reflection height due to the X2.2-class solar flare. The synthetic electric field strength E was calculated as [3]

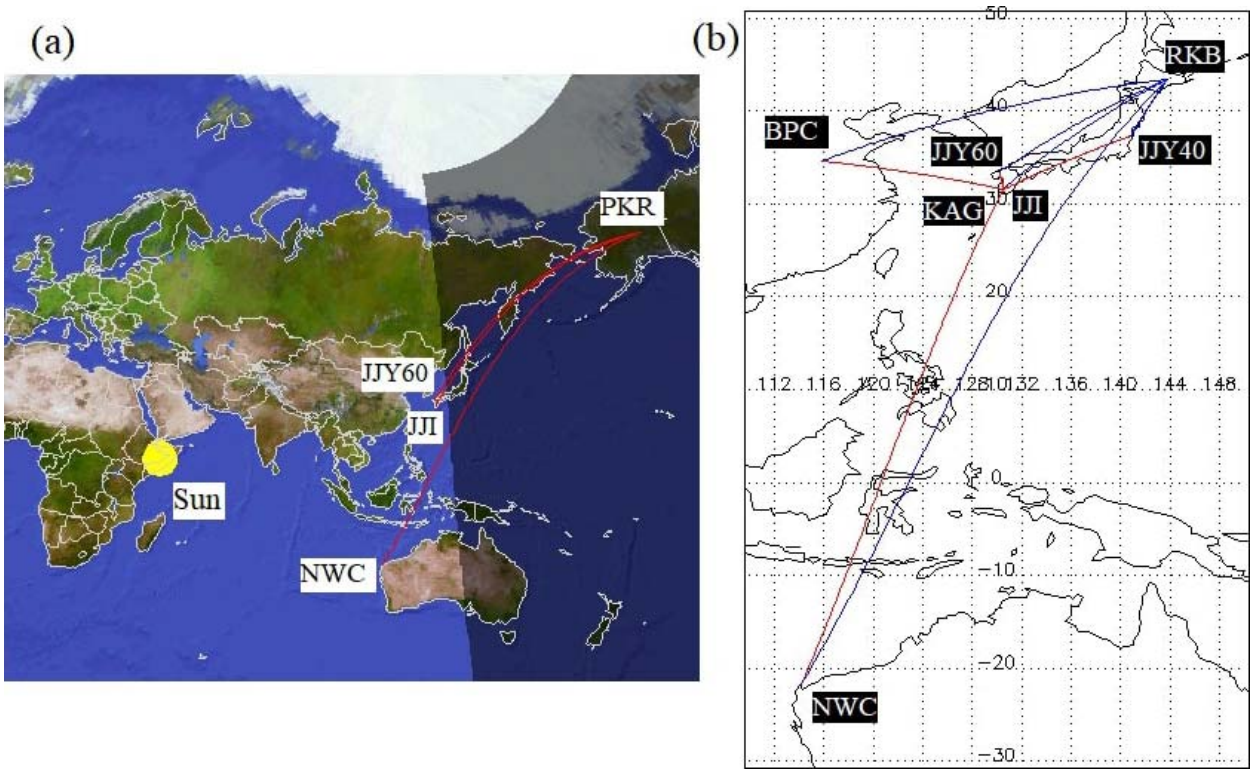

Figure 1. Location of (a) the subsolar point and terminator and (b) VLF/LF paths.

$$E = Eg + \sum_{K=1}^{n} E_{SK} \tag{1}$$

where K is the number of hops. The ground wave Eg was calculated according to

$$Eg = |Eg| \exp(jkGr) \tag{2}$$

where k is the wave number of the VLF/LF signals and Gr is the great circle distance between the transmitter and receiver. The effective field strength of the transmitted sky waves Es_K (mV/m) was calculated for a loop antenna as

$$Es_K = \frac{600\sqrt{Pt}\cos(\psi_K)\prod_{L=1}^{K} Rc_{K,L}\prod_{L=1}^{K-1} Rg_{K,L}}{\sum_{L=1}^{K}(Pl_{K,L})} Fc_K Ft_K Fr_K \exp\left(-jk\sum_{L=1}^{K} Pl_{K,L}\right) \tag{3}$$

where Pt (e.g., 22.5 kW for JJY60) is the radiated power (kW), ψ (=0.11 rad in the case of a one-hop wave for the JJY60-RKB path with a reflection height of 90 km) is the angle of departure and arrival of the sky wave at the ground, L is the number of reflection points from the transmitter, Rc is the ionospheric reflection coefficient, Rg ($\simeq$1.0) is the reflection coefficient of Earth's surface, Fc is the ionospheric focusing factor, Ft is the transmitting antenna factor, Fr is the receiving antenna factor, Pl (e.g., 1619.1 km in the case of a one-hop sky wave for JJY60-RKB path with a reflection height of 90 km) is the path length of each sky wave, and $Rc_{K,L}$ is the ionospheric reflection coefficient of the K-hop sky wave at the Lth reflection point. $L = 1$ for a one-hop sky wave, 1 to 2 for a two-hop sky wave (the hop point near the transmitter is 1, and the hop point near the receiver is 2), 1 to 3 for a three-hop sky wave (one at the transmitter), and 1 to 10 for a 10-hop sky wave. Rc is determined as described in [3] and by an empirical value that depends on the solar zenith angle and transmitter frequency. Fc is also determined by [3] and depends on the horizontal distance between the transmitter and receiver as well as the period (day vs. night). Ft and Fr are determined by Earth's surface (land, sea, or ice), transmitter frequency, and elevation angle according to [3].

Table 1. Solar zenith angle at the midpoints of all paths

Path	Solar zenith angle at midpoints of the path (°)
NWC-KAG	62.3988
BPC-KAG	64.3417
NWC-RKB	68.5437
JJY60-KAG	70.253
JJI-KAG	70.4654
BPC-RKB	70.5001
JJY40-KAG	74.8168
JJY60-RKB	76.0206
JJI-RKB	76.2409
JJY40-RKB	80.1812
JJY60-PKR	98.8006
JJI-PKR	99.2514
NWC-PKR	100.172

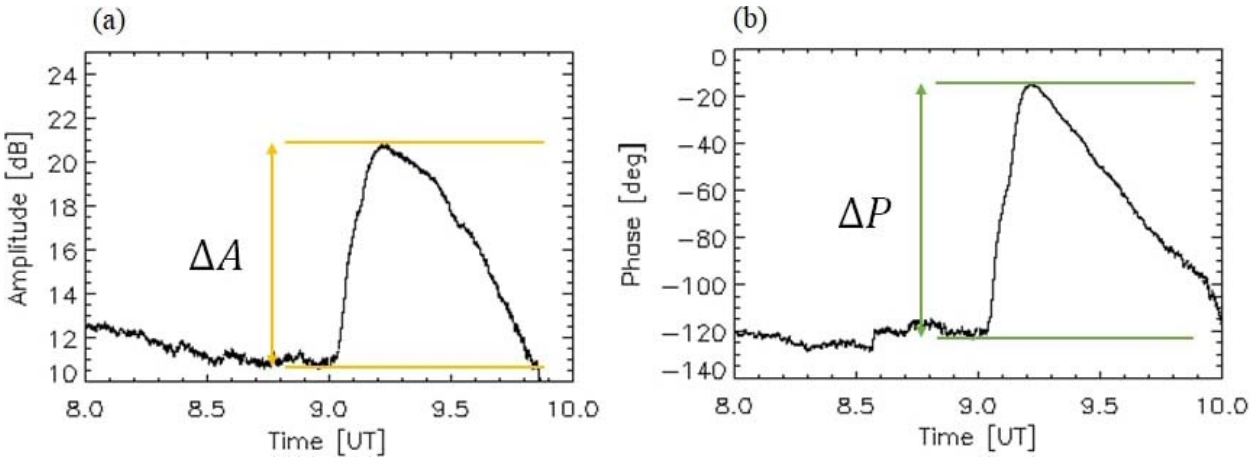

Figure 2. Examples of (a) ΔA and (b) ΔP for the BPC-RKB path.

3. Results and Discussion

Figure 3 shows ΔA and ΔP versus the solar zenith angle at the midpoints of the propagation paths. Among the 13 paths, variations in amplitude and phase were observed in eight and six paths, respectively. Variations in amplitude due to the solar flare were observed in eight of the VLF/LF paths, and there were no variations in amplitude in the remaining five paths. Three of those five paths were completely derived of sunlight, and the other two paths were short (63.9 km and 226.4 km). If the one-hop wave was in antiphase with the two-hop wave, variations due to a solar flare would be canceled. Six of the VLF/LF paths were characterized by phase variations. Phase data for the other seven paths were lacking. As shown in Figure 3, there was no clear trend in ΔA, whereas ΔP increased as the solar zenith angle decreased. In general, the VLF/LF phase showed a one-to-one correspondence with the vertical motion of the reflection height in the D-region ionosphere. A decrease (increase) in reflection height would result in a shorter (longer) path length, and the phase would advance (delay). However, there was no one-to-one correspondence between the VLF/LF amplitude and reflection height because attenuation and interference affected the variations in amplitude, resulting in a non-trend for ΔA. ΔP becomes large for daytime paths, in particular, on the western side near the subsolar point.

The wave-hop method was used to calculated the reduction in reflection height (Δh) from the observed ΔA and ΔP. Figure 4 shows that Δh decreased as the solar zenith angle increased. The solar zenith angle is the angle between the local zenith and the line of sight from the sun; that is, the solar zenith angle is 0° at the subsolar point. The values of the data points in Figure 4 are smaller than those of Figure 3. For five paths of ΔA and one path of ΔP, the Δh calculated based on the wave-hop method did not match the observed ΔA and

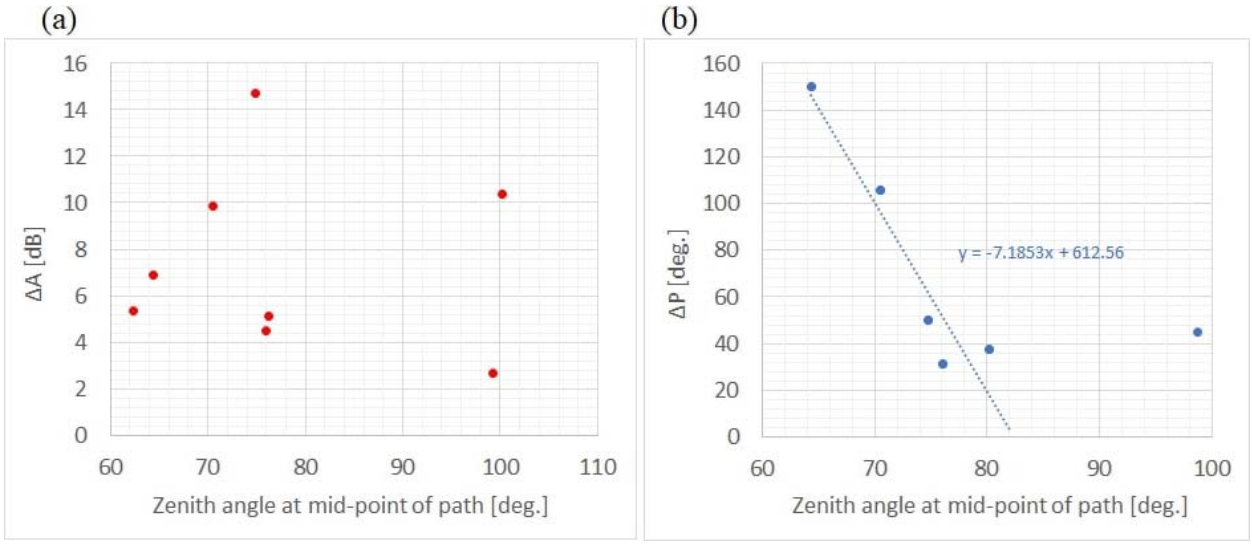

Figure 3. (a) ΔA and (b) ΔP versus the solar zenith angle at the midpoints of the paths.

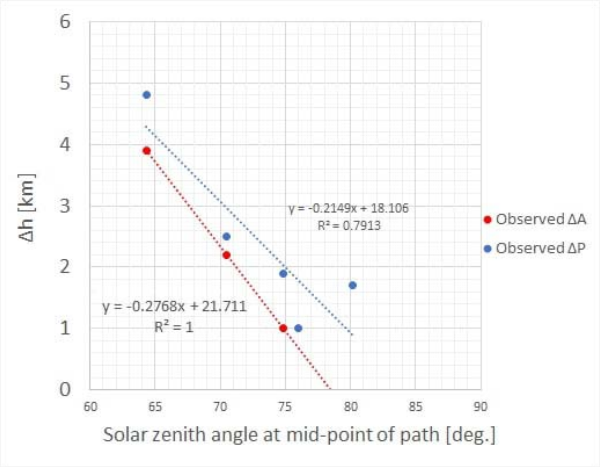

Figure 4. Δh versus the solar zenith angle at the midpoints of the paths.

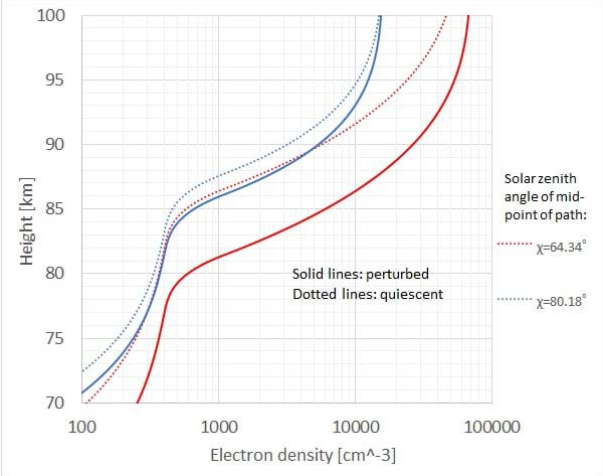

Figure 5. Estimated electron density profiles of two paths based on the IRI-2016 model. The red and blue curves indicate a solar zenith angle (χ) at the midpoints of the path of 64.34° and 80.18°, respectively. The solid and dotted curves indicate the profiles during and before the solar flare, respectively.

ΔP. The electric field strength at the receiver was calculated for the case of $\Delta h = 0$ km to 15 km, but the observed ΔA and ΔP values were not within the range of the calculation results. The disagreement between the observed and calculated values can be attributed to the setting of the reference height in the calculation. Even if the reference height was increased in 0.5 km steps from 77 km (the default value from [3]) to 90 km, a matched point could not be identified. Calculation of Δh requires smaller steps of ≤ 0.1 km because large changes in ΔA occur in response to small differences in the reference height. Here, the Δh estimated from the observed ΔA was different from that determined based on the observed ΔP. The difference in Δh may have been due to the assumed reference height.

The increase in electron density (ΔN) was estimated by the comparison with the Δh estimated from ΔP and International Reference Ionosphere (IRI-2016) model. Figure 5 shows the estimated electron density profiles during and before the solar flare. The electron density during the solar flare increased for two paths, with a larger increase seen in the electron density at $\chi = 64.34°$ than at $\chi = 80.18°$. At a height of 85 km, ΔN at $\chi = 64.34°$ and $\chi = 80.18°$ was 5465.7 cm^{-3} and 200.4 cm^{-3}, respectively. Our results indicate higher electron density in the D-region ionosphere closer to the subsolar point; that is, an inhomogeneity arose from the fact that, during the solar flare, the D-region ionosphere was strongly ionized near the subsolar point but weakly ionized far from the subsolar point.

4. Conclusions

In this study, the horizontal inhomogeneity of the reflection height and electron density in the D-region ionosphere during an X-class solar flare on 6 September 2017 was investigated using multipath VLF/LF transmitter signals of the OCTAVE network.

For eight out of 13 VLF/LF paths, ΔA and ΔP values were in the range of 2.65 dB to 14.73 dB and 31.0° to 150.25°, respectively. Based on the wave-hop method, the estimated Δh (1.0 km to 4.8 km) decreased as the solar zenith angle increased. Based on the IRI-2016 model, at a height of 85 km, ΔN was larger at $\chi = 64.34°$ (5,465.7 cm^{-3}) than at $\chi = 80.18°$ (200.4 cm^{-3}). The inhomogeneity in D-region ionization could be attributed to the solar flare.

5. References

1. J. R. Wait and K. P. Spies, "Characteristics of the Earth-Ionosphere Waveguide for VLF Radio Waves," *NBS Technical Note*, **300**, 1964, pp. 15-18.
2. A. Kumar and S. Kumar, "Solar Flare Effects on D-Region Ionosphere Using VLF Measurements During Low- and High-Solar Activity Phases of Solar Cycle 24," *Earth, Planets and Space*, **70**, 2018, pp. 10-13.
3. International Telecommunication Union, "Recommendation ITU-R P.684-7, Prediction of Field Strength at Frequencies Below 150 kHz," P Series, Geneva, Switzerland, 2016, pp. 2-22.